RSC Advances

This is an *Accepted Manuscript*, which has been through the Royal Society of Chemistry peer review process and has been accepted for publication.

Accepted Manuscripts are published online shortly after acceptance, before technical editing, formatting and proof reading. Using this free service, authors can make their results available to the community, in citable form, before we publish the edited article. This *Accepted Manuscript* will be replaced by the edited, formatted and paginated article as soon as this is available.

You can find more information about *Accepted Manuscripts* in the **Information for Authors**.

Please do not adjust margins

RSC Advances

RSC Advances

ARTICLE

Crystal Structure, Magnetic and Catalytic Oxidation Property of Manganese(III) Tetrakis(ethoxycarbonyl)porphyrin

Hua-Hua Wang [a], Hui-Qing Yuan [a], Mian HR Mahmood [a,b], Yi-Yu Jiang [a], Fan Cheng [a], Lei Shi [c], Hai-Yang Liu * [a]

A new *meso*-tetraalkyl porphyrin manganese complex, 5,10,15,20-tetrakis(ethoxycarbonyl)porphyrinatomanganese (Mn[III]TECPCl), had been prepared and characterized by X-ray structure determination. Mn[III]TECPCl exists as a coordinated dimer in its crystal structure with a weak antiferromagnetic coupling between two Mn(III) ions. The catalytic oxidation of styrene by Mn[III]TECPCl was carried out in acetonitrile. Mn[III]TECPCl was found recyclable with high conversion efficiency when using TBHP as oxidant and the major product was benzaldehyde. Mn[III]TECPCl was also reusable by using PhIO oxidant, but the major products turned out to be phenyl acetaldehyde and styrene epoxide.

Introduction

From a structural viewpoint, synthetic manganese porphyrins resemble the active centre of heme-containing biological systems. Thus, manganese porphyrins are also widely used in the biomimetic studies of cytochrome P-450[1], catalases[2] or other enzymes[3]. However, manganese porphyrins usually undergo oxidative destruction in homogeneous catalytic oxidation systems[4-6]. The oxidative destruction of manganese porphyrin can be significantly improved with electron withdrawing substituents such as *β*-position halogenation[7-9]. The other way to avoid oxidative destruction is by immobilizing the catalysts onto a rigid, inert support such as montmorillonite[10], multiwalled carbon nanotube[11], magnetite nanoparticles[12], metahalloysite[13], resin[14] and silica gel[15]. Assembled manganese porphyrin crystalline micro-sized porous coordination polymers[16] and metal-organic framework (MOF) [17, 18] are also proved robust catalysts. Although these heterogeneous catalysts are recyclable and stable, the synthetic procedure is complicated with limited type of ligands and the catalytic oxidation is time consuming. On the other hand, lots of oxidants such as *t*-butyl hydroperoxide (TBHP)[19], iodosylbenzene (PhIO) [20], iodobenzene diacetate (PhI(OAc)$_2$) [21], *m*-chloroperbenzoic acid (*m*-CPBA) [22], dioxygen[23] and hydrogen peroxide[24] are effective in the manganese porphyrin catalyzed oxidation reaction. Manganese(V)–oxo[25-27], manganese(IV)–oxo[28-30] and Mn[III]-HOOR[31-33] are suggested as the active intermediates. Interestingly, *trans*-dioxo-Mn[V]-

porphyrin is found inert[27].

Meso-substitution has significant effects on the reactivity of metal porphyrin, especially free radicals involved reations[34, 35]. *Meso*-tetraalkyl porphyrins are useful probes for understanding the structure-property relationship of porphyrin molecules[36]. Although tetraalkylporphyrins may be prepared with good yields,[37-39] there is the less reports on the application of manganese tetraalkylporphyrin in catalytic oxidation[40, 41]. 5,10,15,20-tetrakis(ethoxycarbonyl)porphyrin (TECP) is a convenient precursor for porphine[42]. Recently, we have prepared *β*-fluorinated TECP[43]. Here, we wish to report the preparation and catalytic styrene oxidation of manganese(III) TECP (**Scheme 1**, Mn[III]TECPCl). The X-ray crystal structure showed that Mn[III]TECPCl exists as a dimer with plenty of hydrogen bonding interactions. There is a weak antiferromagnetic coupling between two Mn(III) ions in the dimer. The catalytic oxidation of styrene by Mn[III]TECPCl was carried out in acetonitrile solution at room temperature using TBHP and PhIO as oxidants. Mn[III]TECPCl was found recyclable with high conversion efficiency when using these oxidants. Plausible mechanism has been proposed to explain this observation.

a. *Department of chemistry, South China University of Technology, Guangzhou 510641, China. E-mail: chhyliu@scut.edu.cn; Tel. & Fax: +86 020 22236805*
b. *Department of Chemistry, University of Education, Lahore 54770, Pakistan.*
c. *Department of Chemistry, Guangdong University of Education, Guangzhou 510303, China.*
† Electronic Supplementary Information (ESI) available: [Crystal Structure data]. See DOI: 10.1039/x0xx00000x

Scheme 1. Molecule structure of Mn[III]TECPCl and Mn[III]TPPCl.

Please do not adjust margins

Experimental

Materials and methods

All reagents were purchased from commercial sources and used without further purification, unless otherwise mentioned. Styrene was passed through silica gel column prior to use. Electronic spectra were recorded on Hitachi 3900H UV−vis Spectrophotometer in 1 cm optical path length quartz cell at room temperature. Fourier Translation Infrared spectra (FT-IR) were recorded on a Perkin-Elmer spectrophotometer by using KBr pellets. HR−MS spectra were recorded on Bruker maxis impact mass spectrometer with an ESI source. Single-crystal X-ray diffraction data were recorded on a Rigaku R-AXIS SPIDER IP diffractometer with Cu K_α radiation. All cyclic voltammograms (CV) were performed in N,N-dimethylformamide (DMF) solution containing 0.1 M tetrabutylammonium perchlorate (TBAP) and Mn^{III}TECPCl (3 mM) using CHI-660E electrochemical analyzer under nitrogen atmosphere at ambient temperature. The scan rate was 100 mV/s. A three-electrode system consisting of a glassy carbon working electrode, a platinum wire counter electrode and saturated $Ag/AgNO_3$ electrode as the reference electrode were employed. The $Ag/AgNO_3$ electrode contained 1 M TBAP in DMF. Half-wave potentials ($E_{1/2}$) for reversible or quasi-reversible redox processes were calculated as $E_{1/2} = (E_{pa} + E_{pc})/2$, where E_{pa} and E_{pc} represent the anodic and cathode peak potentials, respectively. The $E_{1/2}$ Value for the ferrocene couple under these conditions was 0.47 V. Analysis of oxidation products was recorded by gas chromatograph (Echrom A90) equipped with an Agilent HP-5 capillary column (30.0 m × 320 μm ID: 0.25 μm film thickness) coupled with FID detector. The carrier gas was nitrogen and the chromatographic conditions were as follows: the oven temperature was retained at 60 ^{o}C for 4 min, and then increased at a rate of 10 ^{o}C/min (from 60 to 250 ^{o}C); the injector temperature was set 230 ^{o}C while the detector temperature was kept 250 ^{o}C. The injection volume was 1.0 μL and the products were confirmed by the retention time using standard samples under the same GC conditions. The yields of products were reported with respect to the amount of oxidant used. The solid-state magnetic susceptibility was measured under helium on a Quantum Design PPMS-9 magnetometer from 2 to 300 K at a field of 1 T. The powder sample was installed in the parafilm and the magnetic moment was obtained after background correction. The experimental susceptibilities were corrected for the diamagnetism of the constituent atoms (Pascal's table).

Synthesis of catalysts

The metalloporphyrin catalysts 5,10,15,20-tetrakis(ethoxycarbonyl)porphyrin manganese(III) chloride (Mn^{III}TECPCl) and 5,10,15,20-tetraphenylporphyrin manganese(III) chloride (Mn^{III}TPPCl) (**Scheme 1**) were prepared using literature procedures[44, 45]. The synthesis of 5,10,15,20-tetrakis(ethoxycarbonyl)porphyrin ligand (TECP) was performed by our recently reported procedure[43].
Mn^{III}TECPCl was obtained by refluxing TECP with $Mn(OAc)_2·4H_2O$ in DMF solution for 2 h. After that it was

diluted with CH_2Cl_2 and washed with saturated aqueous solution of NaCl and HCl several times. The organic layer was collected and dried over anhydrous Na_2SO_4. The filtrate was concentrated and the crude product was purified on silica gel (100−200 mesh) using CH_2Cl_2/CH_3OH (95:5 v/v) as eluent. Black solid was obtained after recrystallization from CH_2Cl_2/hexane (1:4 v/v). Yield: 85 %. UV−vis (CH_2Cl_2) λ_{max} (log ε): 364 (4.80), 474 (4.90), 570 (4.07); HR−MS (ESI) ($[M−Cl]^+$): calcd for $C_{32}H_{28}MnN_4O_8$ 651.1282, found 651.1285, with an isotope distribution pattern the same as the calculated one.

X-ray Diffraction Studies of Mn^{III}TECPCl

A suitable crystal was selected and measurement on an Xcalibur, Sapphire3, Gemini ultra diffractometer using Cu K_α radiation. The crystal was kept at 150(5) K during data collection. Using Olex2[46], the structure was solved with the olex2.solve structure solution program using Charge Flipping and refined with the XL[47] refinement package using Least Squares minimization. All non-hydrogen atoms of the complex were refined anisotropically. The hydrogen atoms were generated by the riding mode. Data collection and structural refinement parameters are given in **Table 1**. CCDC 1059156 contained the supplementary crystallographic data for Mn^{III}TECPCl.

Table 1. Crystal data and structure refinement for Mn^{III}TECPCl.

Compound	Mn^{III}TECPCl
Empirical formula	$C_{32}H_{28}N_4O_8MnCl$
Formula weight	686.97
Temperature /K	150(5)
Crystal system	monoclinic
Space group	$P2_1/c$
a /Å	14.9631(3)
b /Å	9.6880(3)
c /Å	21.4177(5)
α /°	90.00
β /°	100.638(2)
γ /°	90.00
Volume /Å3	3051.41(13)
Z	4
ρ_{calc} g/cm^3	1.495
μ /mm^{-1}	4.832
F(000)	1416.0
Radiation	Cu $K\alpha$ (λ = 1.54184 Å)
Reflections collected	10067
Independent reflections	4591 [R_{int} = 0.0372, R_{sigma} =0.0453]
Data/restraints/parameters	4591/0/527
Goodness-of-fit on F^2	1.049
Final R indexes [I>=2σ (I)]	R_1 = 0.0400, wR_2 = 0.1002
Final R indexes [all data]	R_1 = 0.0447, wR_2 = 0.1044
Largest diff. peak/hole / e Å-3	0.50/-0.42

General Procedure for Catalytic Oxidation

A mixture of organic substrate (1.0 mmol), oxidant (0.1 mmol) and catalyst (1.0 μmol) in 2 mL acetonitrile was stirred in a 10 mL glass flask at room temperature. After an appropriate reaction time, chlorobenzene (5.0 μL) was added to this

reaction mixture as internal standard. The conversion efficiency and selectivity were monitored by GC analysis.

Typical procedure for the reuse of catalyst in the catalytic oxidation of styrene

A mixture of catalyst (1.0 μmol), styrene (1 mmol) and TBHP (0.1 mmol) in CH$_3$CN (2 mL) was sealed in a 10 mL glass flask, evaporated under vacuum after stirring at room temperature for 2.5 h. The resulting solid was washed with hexane for several times, and detected by GC analysis. The recovered catalyst solid was used in the successive run.

The stability of catalyst

A mixture of Mn^{III}TECPCl and oxidant in 2 mL acetonitrile was stirred in a 10 mL glass flask at room temperature. After an appropriate reaction time, 100 μL of the mixture was diluted to 3 mL acetonitrile solution in a quartz cell with 1 cm optical path length and UV−vis spectrum was obtained.

Results and discussion

X-ray structure of Mn^{III}TECPCl

Single crystal of Mn^{III}TECPCl, suitable for X-ray diffraction analysis, was obtained by slow evaporation of dichloromethane/hexane solution. Single crystal of Mn^{III}TECPCl was monoclinic in the space group $P2_1$/c, with nonplanar porphyrin core, like Mn(III) tetraphenylporphyrin[48]. The molecular structure of Mn^{III}TECPCl is depicted in **Fig. 1a**. The 24-membered macrocyclic core of the porphyrin is coplanar, and the displacement of each atom in the equatorial mean plane is within 0.15 Å. The distance between the Mn^{3+} ion to the mean plane is 0.1701 Å. The six-coordinate manganese atom located at the centre of this porphyrin macrocycle and is bonded to four nitrogen, one chlorine and one oxygen atom to construct a distorted octahedral. Two manganese porphyrin molecules combined in a dimer (**Fig. 1b**) and two manganese porphyrin core planes are parallel with a distance of 3.2845 Å, indicating the existence of π−π stacking, in addition to coordination interactions. The short intermacrocycle distances are the consequence of two supplementary structural features. The first one is weak coordination bond between manganese ion and oxygen atom from another macrocycle. The second one is the nearly coplanar orientation of the *meso*-5,10,15,20-tetra-ethoxycarbonyl groups towards the macrocycle, which facilitates the intermolecular approach, despite their spatial proximity. This distance is comparable to the same *meso*-ethoxycarbonyl groups corrole free base[49].
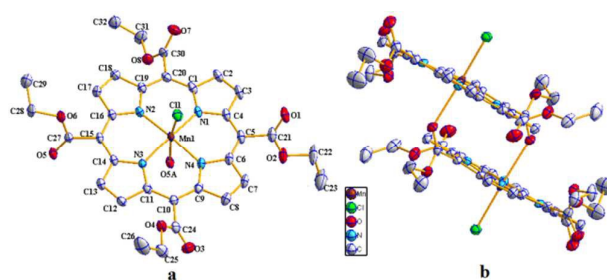
Fig. 1. ORTEP plots of Mn^{III}TECPCl. (a) Monomer. (b) Dimer. (Showing 50% probability thermal displacement ellipsoids, hydrogen atoms are omitted for clarity).

Selected bond distances and angles for Mn^{III}TECPCl are listed in **Table 2**. The Mn-N bond length range from 2.0159(2) Å to 2.0275(2) Å with an average value of 2.0224(9) Å, and the Mn-Cl bond length is 2.4235(8) Å, both of the bond length were comparable to 5,10,15,20-tetrakis(4-hydroxyphenyl) porphyrin manganese chloride (Mn^{III}TOHPPCl) or Mn^{III}TPPCl found in the literature[48, 50]. The Mn-O bond length is 2.6290(2) Å, and is weaker than covalent bond (2.16 Å).

Table 2. Selected bond distances (Å) and bond angles (°) for Mn^{III}TECPCl.

Bond distances (Å)			
Mn1-Cl1	2.4235(7)	Mn1-N1	2.0270(2)
Mn1-N2	2.0275(19)	Mn1-N3	2.0200(19)
Mn1-N4	2.0160(2)	Mn1-O5A	2.6290(2)
Bond angles (°)			
N3-Mn1-Cl1	94.65(6)	N3-Mn1-N1	169.66(8)
N3-Mn1-N2	89.33(8)	N1-Mn1-Cl1	95.69(6)
N1-Mn1-N2	88.91(8)	N4-Mn1-Cl1	90.72(6)
N4-Mn1-N3	89.67(8)	N4-Mn1-N1	90.38(8)
N4-Mn1-N2	170.48(8)	N2-Mn1-Cl1	98.79(6)
C14–N3–Mn1	127.23(16)	C11–N3–Mn1	126.80(15)
C1–N1–Mn1	127.91(16)	C4–N1–Mn1	126.14(17)
C6–N4–Mn1	125.65(17)	C9–N4–Mn1	126.80(16)
C19–N2–Mn1	127.32(15)	C16–N2–Mn1	126.55(16)

Hydrogen bonding plays an important role in constructing multi-dimensional structure as well as in catalytic oxidation[50]. **Fig. 2** shows the packing of Mn^{III}TECPCl constructed from hydrogen bonding. Apparently, there are two types of hydrogen bonding i.e. intramolecular and intermolecular bonding. The former exists between oxygen of carbonyl and hydrogen of pyrrole, which was also observed in the *meso*-ethoxycarbonyl groups corroles[49]. While the latter exists between the oxygen of the ester group from one manganese porphyrin and hydrogen of pyrrole or ethyl group from another manganese porphyrin.
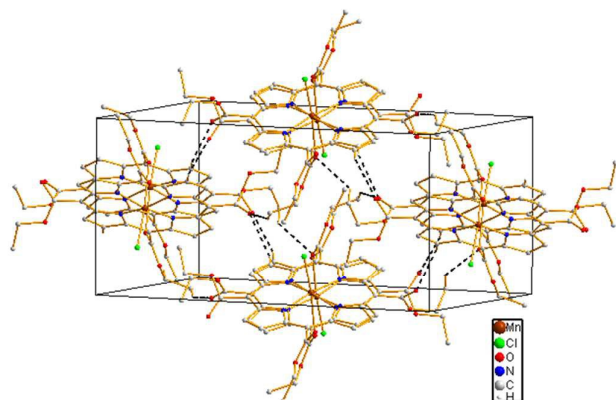
Fig. 2. Unit cell of Mn^{III}TECPCl show hydrogen bonding interaction. Hydrogen atoms not involved in these contacts are omitted for clarity.

Magnetic properties

Magnetic data for Mn^{III}TECPCl are reported in **Fig. 3** in the form of χ_m and μ_{eff} versus T. The value of μ_{eff} varies from 4.66 μ_B at 300 K to 3.35 μ_B at 2 K. The magnetic moment clearly shows a platform ($\sim$4.64 μ_B) at high temperatures (300–38 K). With decreasing the temperature, the μ_{eff} decreases slowly and reaches its terminal value of 4.48 μ_B at about 12 K, and after this the μ_{eff} decrease rapidly and reaches its lowest value of $\sim$3.35 μ_B at 2 K. The abrupt μ_{eff} rise in the range of temperature $2 < T < 12$ K is characteristic of a compound with significant zero-field splitting (ZFS) [51]. The effective magnetic moment of 4.66 μ_B at room temperature is lower than the spin-only moment of 4.9 μ_B for an S = 2 system, consistent with other high spin Mn(III) complexes in which g < 2. The magnetic susceptibilities of Mn^{III}TECPCl in the whole temperature range obeys Curie–Weiss law with small negative Weiss constant θ = -0.91 K and Curie constant C = 2.71 emu K mol^{-1}, indicating the occurrence of weak antiferromagnetic interactions in Mn^{III}TECPCl.
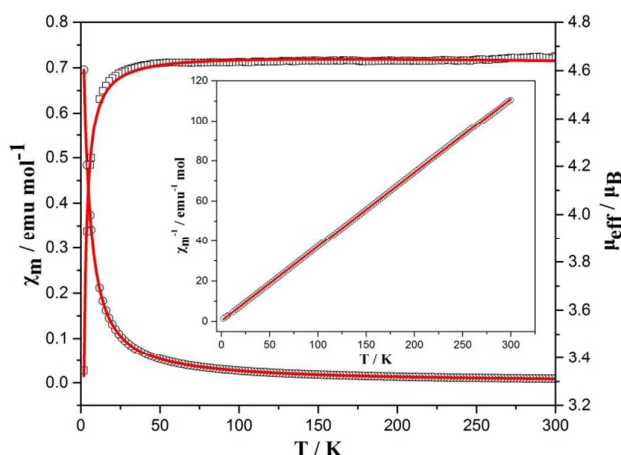
Fig. 3. Temperature dependence of magnetic susceptibility in the forms of μ_{eff} and χ_m versus T for Mn^{III}TECPCl at 1 T between 2 and 300 K. The red solid lines represent the best-fitting results. Inset: Temperature dependence of the magnetic susceptibility in the form of χ_m^{-1} versus T for Mn^{III}TECPCl between 2 and 300 K. The solid line was obtained from the best fit by the Curie−Weiss expression.

The molecular structure of Mn^{III}TECPCl shows that the metal (Mn) centers are linked by weak O5A–Mn coordination bonds to form a dimer (**Fig. 1**), and such interactions are able to transmit magnetic interactions. On the basis of the binuclear Mn^{III}–Mn^{III} (S=2 and 2) model, the magnetic susceptibilities for Mn^{III}TECPCl can be fitted by equation 2 derived from the isotropic exchange spin Hamiltonian (Eq. 1)[52, 53].

$$\hat{H} = -2J\hat{S}_{Mn}\hat{S}_{Mn} + D\hat{S}_{zMn}^2 \quad \text{(Eq. 1)}$$

$$\chi_m = \frac{0.3749}{T}g_{eff}^2\left\{p\cdot\frac{1}{3}\left[\frac{8+2e^{3y}+\frac{1}{y}\left(-\frac{8}{3}-\frac{28}{3}e^{3y}+12e^{4y}\right)}{2+2e^{3y}+e^{4y}}\right]+\right.$$
$$\left.q\left[\frac{2e^{2x}+10e^{6x}+28e^{12x}+60e^{20x}}{1+3e^{2x}+5e^{6x}+7e^{12x}+9e^{20x}}\right]+(1-p-q)\times 2.917\right\}+\text{TIP} \quad \text{(Eq. 2)}$$

where, $y = 1.44\frac{D\,(cm^{-1})}{T}$, $x = 1.44\frac{J\,(cm^{-1})}{T}$ and $\mu_{eff} = 2.828\sqrt{\chi_m T}$.

The term p (or q) is the fraction of Mn(III) [or Mn(III)-Mn(III) dimer], g_{eff} is the effective g value, TIP is the temperature independent paramagnetism. J is the coupling exchange parameter and D is the parameter which describes the effects of the axial field. The best fits, as represented in **Fig. 3**, gave the values g_{eff} =1.75, p = 0.70, D = 7.34 cm^{-1}, q = 0.08, $2J$ = -0.84 cm^{-1} and TIP = -2.7×10^{-4} cm^3/mol, with an agreement factor R of 0.61%, showing the high reliability of data. The R value is defined as[52]

$$R = \sum(\chi_{obsd}T - \chi_{cald}T)^2 / \sum(\chi_{obsd}T)^2 \times 100\% \quad \text{(Eq. 3)}$$

The small negative J value ($|J| < 20$ cm^{-1})[53] suggests a weak antiferromagnetic coupling between the Mn(III) and Mn(III) connected by the coordination bridge. Within the dimer, Mn···Mn separation of 6.56 Å in Mn^{III}TECPCl precludes direct metal–metal bonding, the superexchange through O5A−Mn coordination bonding in the Mn(III)···Mn(III) dimer must be responsible for this antiferromagnetic interaction. The shortest interdimer Mn···Mn distance of 10.53 Å in Mn^{III}TECPCl indicates that interdimer interactions are negligible. This is similar to the previous observation for Mn(2-NC$_3$H$_5$NCTPP)Br complex, in which the antiferromagnetic coupling constant J between Mn(III)-Mn(III) ions is -0.02 cm^{-1} with an intradimer Mn···Mn separation of 8.177 Å linked by C−H···Br hydrogen bonding[52].

Electrochemistry

The electrochemical characteristics of Mn^{III}TECPCl and Mn^{III}TPPCl were investigated by cyclic voltammetry in DMF solutions. **Fig. 4** represents the cyclic voltammograms of Mn^{III}TECPCl and Mn^{III}TPPCl in DMF containing 0.1 M TBAP and ferrocene as internal standard. Manganese porphyrins show a single one-electron reversible or quasi-reversible oxidation and a series of irreversible reductions within the scan window (-2.0 to 2.0 V). Mn^{III}TECPCl exhibits four redox couples located at $E_{1/2}$ = -1.831, -1.531, -0.96 and 0.021 V. The voltammogram is in close resemblance to that of Mn^{III}TPPCl, which exhibits the same redox couples located at $E_{1/2}$ = -1.948, -1.836, -1.310, -0.19 V respectively. The electrochemical properties of manganese porphyrins are well documented in the literature[54-56]. Here, the assignments of Mn^{III}TECPCl redox couples are

made accordingly. The redox couple at $E_{1/2}$ = 0.021 V may be assigned to Mn(III)/Mn(II). The other more negative potential redox couples at $E_{1/2}$ = -0.96, -1.53 and -1.83 V are assigned to porphyrin ring-centered redox processes related to formation of Mn(II) π-anion radical, π-dianion and π-trianions radicals species. The Mn(III)/Mn(II) redox couple of Mn[III]TPPCl appeared at more negative $E_{1/2}$ (-0.19 V). This suggests Mn[III]TECPCl may have a higher stability and catalytic oxidation activity than Mn[III]TPPCl. In addition, an additional oxidation process was observed at $E_{1/2}$ = 1.64 V for Mn[III]TPPCl, which is assigned to the formation of the porphyrin radical cation[57, 58]. This redox peak was not observed for Mn[III]TECPCl within the same electrochemical window, possibly because of the electron-deficient virtue of Mn[III]TECPCl.
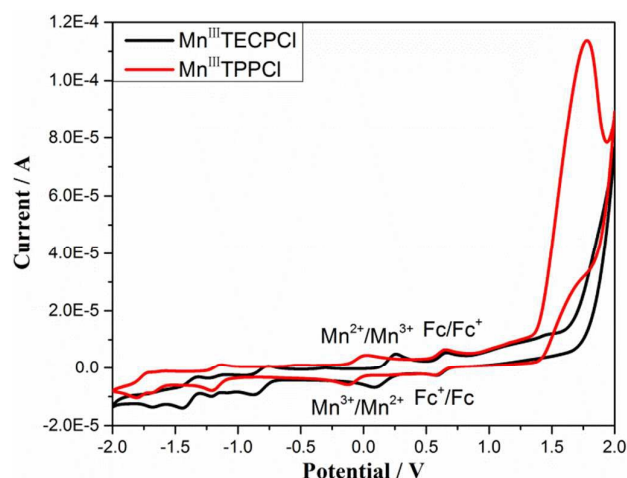
Fig. 4. Cyclic voltammograms of Mn[III]TECPCl and Mn[III]TPPCl in DMF containing 0.1 M TBAP, scan rate = 0.1 V/s. (Ferrocene as internal standard)

Catalytic oxidation activity

It is well documented that high-valent metalloporphyrins having electron-withdrawing groups at the four *meso* positions are efficient oxidation catalysts[59]. Styrene is a commonly used substrate[23, 60, 61]. Previous literatures and our group studies showed that acetonitrile is an ideal solvent for manganese catalysed oxidation of organic substrate[19, 45, 62]. Here, the catalytic oxidation of styrene was carried out in acetonitrile with different oxidants at room temperature. The main oxidation products are benzaldehyde (BA), phenyl acetaldehyde (PA) and styrene epoxide (SO).

Table 3. Catalytic oxidation of styrene by manganese porphyrins.

Entry[a]	Oxidant	Catalyst	Product yield %			
			BA	PA	SO	Total
1	none	Mn[III]TECPCl	0	0	0	0
2	m-CPBA	Mn[III]TECPCl	0.72	14.00	17.43	32.15
3		Mn[III]TPPCl	1.32	2.62	6.48	10.42
4	PhIO	Mn[III]TECPCl	4.67	37.56	33.31	75.54
5		Mn[III]TPPCl	3.20	29.68	41.37	74.25
6		Mn[III]TECPCl	71.47	3.25	14.73	89.45
7[b]	TBHP	Mn[III]TECPCl	37.01	1.63	11.07	49.71
8		Mn[III]TPPCl	42.40	1.57	3.68	47.65

a. Reaction conditions: catalyst (0.001 mmol), oxidation (0.1 mmol), styrene (1 mmol) in 2 mL acetonitrile stirring at room temperature. Yield and selectivity of product were detected by GC, chlorobenzene as internal standard; b. Under argon atmosphere.

The nature and the relative yields of the products formed by catalytic oxidation of styrene using porphyrins vary considerably depending on the catalyst and oxidant. In this work, three oxidants TBHP, *m*-CPBA and PhIO were used, and the experimental conditions were kept the same in all catalytic reactions. In the absence of oxidant, no any products could be detected (**Table 3**, entry 1). When using *m*-CPBA or PhIO as oxidant, the main products are phenyl acetaldehyde (PA) and styrene epoxide (SO) (**Table 3**, entry 2 to 5), similar to the previously reported catalytic oxidation of styrene by *β*-brominated manganese porphyrins[7]. PhIO or *m*-CPBA is a single-oxygen donor and favors the formation of the high-valent (oxo)manganese species Mn[IV]=O,[29] which is responsible for oxygen insertion into the carbon–carbon double bond of styrene. When using TBHP as oxidant, the main product was benzaldehyde (**Table 3**, entry 6), which may be attributed to free radical involved oxidation[63-65]. The yield of benzaldehyde and total oxidation yield was significantly lowered under argon (**Table 3**, entry 7), further confirming Mn[III]TECPCl/TBHP system inclines to free radical involved oxidation[45]. For all tested oxidants, the catalytic activity of Mn[III]TECPCl was observed much higher than control Mn[III]TPPCl, this may be rationalized by the electron-withdrawing effect of the four *meso*-ethoxycarbonyl groups in Mn[III]TECPCl, which leads to a higher catalytic activity. This may also be confirmed from the anticathode shift of its Mn^{3+}/Mn^{2+} couple as compared to Mn[III]TPPCl (**Fig. 4**).
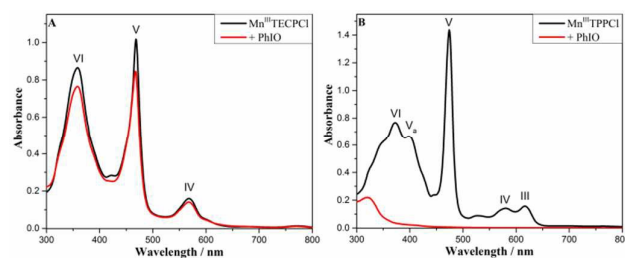
Fig. 5. UV–vis spectra changes of Mn[III]TECPCl (A) and Mn[III]TPPCl (B) upon the addition of PhIO in CH₃CN solution (Reaction time 2.5 h. [PhIO]/[catalyst] = 100:1.)

It is known the periphery electron-withdrawing group will not only enhance the catalytic activity of metalloporphyrin, but also its anti-oxidation stability[59]. To check the anti-oxidation stability of Mn[III]TECPCl, direct reaction of catalysts with PhIO and TBHP were carried out and the reaction were monitored by UV-Vis spectroscopy. As shown in **Fig. 5**A, Mn[III]TECP displays classical electronic spectra of manganese porphyrin spectrum. Its UV-Vis characteristics may well be depicted using Gouterman's four-orbital model[66]. Electronic spectra of Mn[III]TPPCl (**Fig. 5**B) has been assigned in earlier publication[67]. Soret peak VI (372 nm) is originated from a_{1u}, $a_{2u} \rightarrow e_g*$ and a'_{2u}, $b_{2u} \rightarrow e_g$ transitions. Soret peak V_a (398 nm) is LMCT band from $a'_{2u} \rightarrow a_{1g}$ transition. The sharp absorption peak V (474 nm) is the typical LMCT band assigned to a'_{2u}, $b_{2u} \rightarrow e_g$ transition. The less intense Q bands IV (580 nm) is from a_{1u}, $a_{2u} \rightarrow e_g*$ transition, and III (617 nm) is LMCT band from a_{1u}, $a_{2u} \rightarrow e_g$ transition. Mn[III]TECPCl exhibits similar absorption peaks at 358 nm (VI), 468nm (V) and 568 nm (IV) respectively. Due to the substituent effect, V_a and III peaks could not be resolved clearly in the UV-Vis spectra of Mn[III]TECPCl. Which is quite similar to the case of chloro(aquo)etioporphyrinI manganese(III) complex[67]. As compared to Mn[III]TPPCl, the electronic spectrum of Mn[III]TECPCl is obviously blue-shifted. This may be rationalized by the electron-deficient property of porphyriniod macrocycle[68]. When PhIO oxidant was added to the catalyst solution, Mn[III]TPPCl was completely destructed after 2.5 hours as indicated by UV-Vis spectrum (**Fig. 5**B). While only about 12% Mn[III]TECPCl decomposed at the same condition (**Fig. 5**A). Interestingly, when using TBHP as oxidant, nearly no decomposition of Mn[III]TECPCl could be observed even after 12.5 hours with [TBHP]/[catalyst] = 500:1 (**Fig. 6**A). In this situation, although the stability of Mn[III]TPPCl was also observed greatly enhanced, the oxidative destruction Mn[III]TPPCl was still very obvious as indicated by the intensity loss of the absorption peaks (**Fig. 6**B).
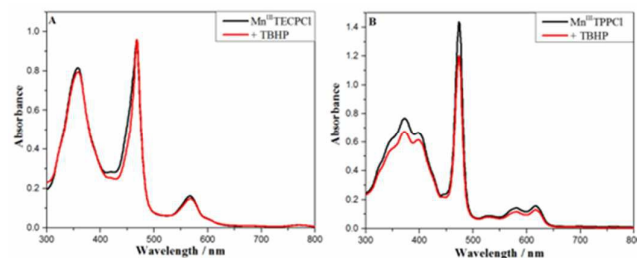
Fig. 6. UV–vis spectra changes of Mn[III]TECPCl (A) and Mn[III]TPPCl (B) upon the addition of TBHP in CH₃CN solution (Reaction time 12.5 h. [TBHP]/[catalyst] = 500:1.)

These observations prompted us to explore the recovery or reuse of Mn[III]TECPCl under the catalytic reaction conditions using TBHP and PhIO oxidatns (**Fig. 7**). After five cycles, the total oxidation products yield by Mn[III]TECPCl was kept above 70% for both oxidants. This indicates *meso*-ethoxycarbonyl groups were a good alternative to stabilize manganese porphyrin in resisting oxidation. The IR spectra of recovered Mn[III]TECPCl is the same to original catalyst (**Fig. 8**), suggesting Mn[III]TECPCl is very stable in the catalytic reactions.
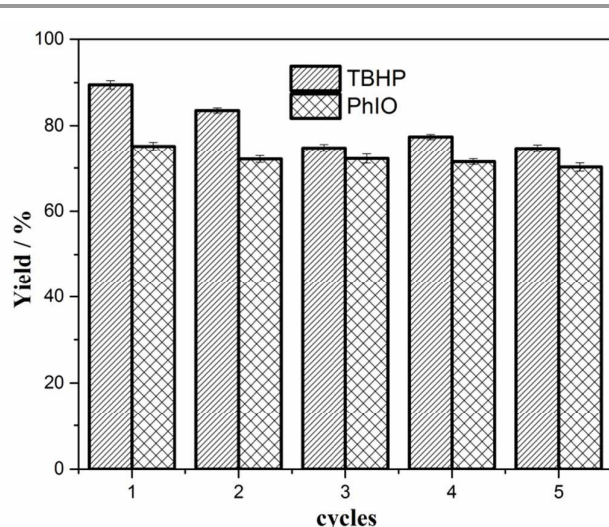
Fig. 7. The total oxidation products yield changes of Mn[III]TECPCl catalyst with the different oxidants and cycles. (Reaction condition: catalyst/oxidant/styrene = 1:100:1000 in 2 mL CH₃CN, catalyst: 1μM, products were analyzed by GC after 2.5 h)
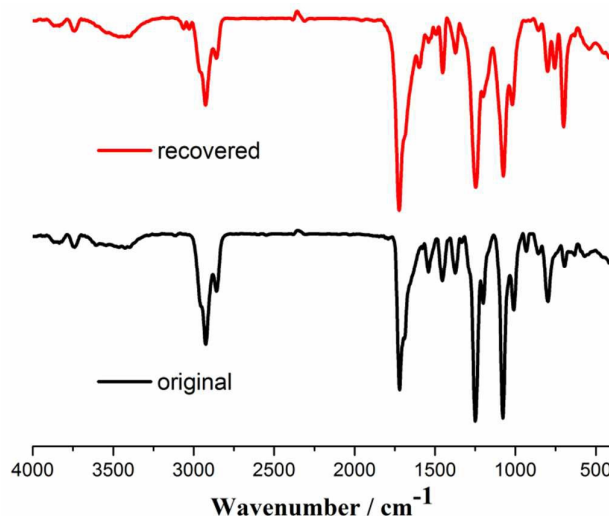
Fig. 8. FT-IR spectra (KBr pellets) of recovered and original Mn[III]TECPCl catalyst.

Mechanistic Considerations

Manganese porphyrins possess high catalytic activity in alkene epoxidation using PhI(OAc)₂[21], PhIO[7] and *m*-CPBA[22] oxidants. Epoxides are generally considered from the oxygen atom transfer (OAT) reaction of high-valent (oxo)manganese porphyrin and alkene[27]. It has been observed manganese porphyrin catalyzed oxidation of styrene by TBHP oxidant gave benzaldehyde as main product[19]. Three types of reactive species have been postulated for manganese porphyrin catalyzed oxidation reactions: porphyrin manganese(IV)–oxo[28], porphyrin manganese(V)–oxo[26] and porphyrin Mn[III]–HOOR[31-33]. Porphyrin manganese(V)–oxo is a transient species, it return

back to manganese(III) via manganese(IV)–oxo in a few minutes[21, 25, 69].
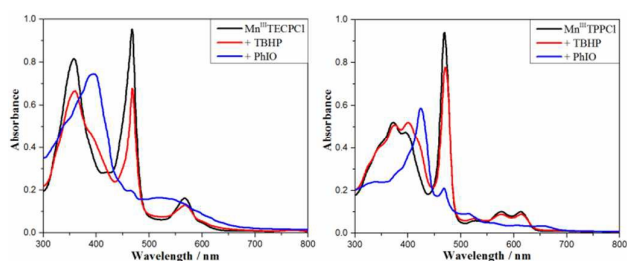
Fig. 9. UV–vis spectra changes of Mn^{III}TECPCl (left) and Mn^{III}TPPCl (right) upon the addition of TBHP and PhIO in acetonitrile. [Mn porphyrin] / [Oxd] = 1/10.

To check the possible active species involved, direction reaction the manganese porphyrin with TBHP and PhIO were monitored by UV-Vis spectra (**Fig. 9**). In the presence of TBHP, there was no obvious change in the spectrum, except a small new shoulder peak appeared at soret band and obvious decrease in the absorption intensity. Similar spectral changes were observed for Mn^{III}TPPCl too. This spectra change may be ascribed to the formation of Mn^{III}–HOOR. In the presence of PhIO, the UV-vis spectra of Mn^{III}TECPCl exhibited a new soret band at 387 nm and the MLCT (metal to ligand charge transfer) band at around 475 nm disappeared, indicating the formation of high-valent porphyrin Mn^{IV}=O intermediate[31]. Similar phenomena were observed for Mn^{III}TPPCl. From these observations, it can be concluded that Mn^{III}TPPCl and Mn^{III}TECPCl react with PhIO yield high-valent Mn^{IV}=O intermediate, while TBHP coordinates to the porphyrin manganese metal centre to form axial ligated complexes. As the main product is benzaldehyde in styrene/Mn^{III}TECPCl/TBHP system and there is no spectroscopic sign that the reaction of Mn^{III}TECPCl and TBHP will generate porphyrin Mn^{IV}=O intermediate. We suggest here the catalytic oxidation of styrene by TBHP is a free-radical involved process[70]. *p*-Benzoquinone (*p*-BQ) is a well-known reactive oxygen radical species (RORS) trapping agent[71]. When *p*-BQ was added to the styrene/Mn^{III}TECPCl/TBHP system, the catalytic oxidation reaction was totally suppressed (**Fig. 10**), indicating RORS were indispensable active intermediate. When using PhIO as oxidant, the addition of *p*-BQ will also lower the total product

yield remarkably. This suggests RORS is also involved in the oxidation of styrene by PhIO. Interestingly, *p*-BQ cannot suppress the styrene oxidation completely when using Mn^{III}TPPCl catalyst and TBHP oxidant. When using PhIO as oxidant, the catalytic activity of Mn^{III}TPPCl was not inhibited as much as that of Mn^{III}TECPCl. This shows the catalytic pathway not only depends on the oxidant, but the virtue of the catalyst also. Detailed mechanism still needs further investigation.
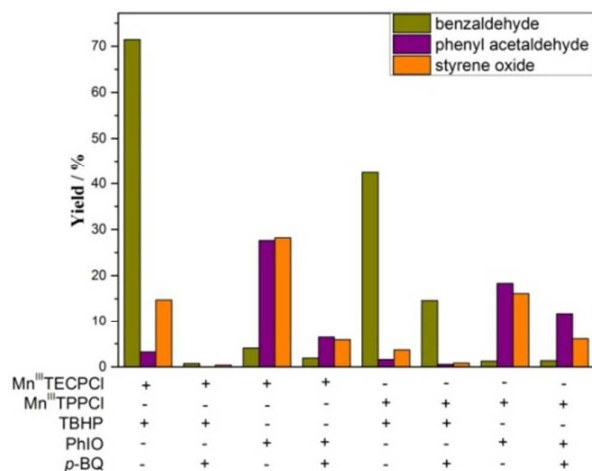
Fig. 10. Change in the yield of products after adding *p*-BQ in different catalysts/oxidants systems. (+ = present; - = absent)

The plausible mechanism of styrene oxidation catalyzed by manganese porphyrin is depicted in **Scheme 2**. The reaction between TBHP and Mn^{III}TECPCl or Mn^{III}TPPCl gives Mn^{III}-HOOR intermediate, which undergo heterolysis to form RORS which oxidizes styrene to give BA, PA and SO. When using PhIO as oxidant, porphyrin Mn^{IV}=O formed and subsequently transfers its oxygen to the carbon–carbon double bond of styrene to form SO and PA. An alternate pathway is that Mn^{IV}=O reacts with styrene to give radical intermediate which will initiate oxygen involved free radical chain propagation reaction[28, 29].
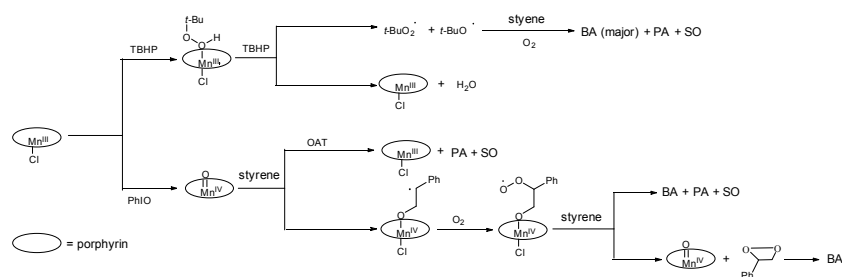
Scheme 2. Plausible mechanism for oxidation of styrene by Mn^{III}TECPCl.

Conclusions

In summary, we have reported the synthesis, structure characterization, magnetic properties of Mn^{III}TECPCl, and its

catalytic activities for styrene in CH₃CN in homogenous system. In its crystal, Mn^{III}TECPCl is linked through O–Mn coordination bonds to form dimer, and displays weak antiferromagnetic intradimer coupling between Mn(III) ions. As compared to tetra-aryl manganese porphyrin Mn^{III}TPPCl, Mn^{III}TECPCl exhibits better catalytic activity and anti-oxidation capacity. Mn^{III}TECPCl can be recycled with high catalytic activity even after five cycles in the oxidation of styrene by TBHP and the plausible reactive intermediate is reactive oxygen radical species generated from the heterolysis of porphyrin Mn^{III}-HOOR. Mn^{III}TECPCl was also reusable in the oxidation of styrene by using PhIO oxidant.

Acknowledgements

References

1. D. Mansuy, *Coord. Chem. Rev.*, 1993, **125**, 129-141.
2. H. Srour, P. Le Maux, S. Chevance and G. Simonneaux, *Coord. Chem. Rev.*, 2013, **257**, 3030-3050.
3. I. Batinic-Haberle, Z. Rajic, A. Tovmasyan, J. S. Reboucas, X. D. Ye, K. W. Leong, M. W. Dewhirst, Z. Vujaskovic, L. Benov and I. Spasojevic, *Free Radic. Bio. Med.*, 2011, **51**, 1035-1053.
4. D. Mansuy, *Pure Appl. Chem.*, 1990, **62**, 741-746.
5. B. Meunier, *Chem. Rev.*, 1992, **92**, 1411-1456.
6. D. Dolphin, T. G. Traylor and L. Y. Xie, *Acc. Chem. Res.*, 1997, **30**, 251-259.
7. D. C. d. Silva, G. DeFreitas-Silva, E. d. Nascimento, J. S. Rebouças, P. J. S. Barbeira, M. E. M. D. d. Carvalho and Y. M. Idemori, *J. Inorg. Biochem.*, 2008, **102**, 1932-1941.
8. E. d. Nascimento, G. d. F. Silva, F. A. Caetano, M. A. M. Fernandes, D. C. da Silva, M. E. M. D. de Carvalho, J. M. Pernaut, J. S. Rebouças and Y. M. Idemori, *J. Inorg. Biochem.*, 2005, **99**, 1193-1204.
9. S. Rayati, S. Zakavi, E. Bohloulbandi, M. Jafarian and M. R. avei, *Polyhedron*, 2012, **34**, 102-107.
10. A. M. Machado, F. Wypych, S. M. Drechsel and S. Nakagaki, *J. Colloid Interface Sci.*, 2002, **254**, 158-164.
11. A. Rezaeifard and M. Jafarpour, *Catal. Sci. Technol.*, 2014, **4**, 1960-1969.
12. M. S. Saeedi, S. Tangestaninejad, M. Moghadam, V. Mirkhani, I. Mohammadpoor-Baltork and A. R. Khosropour, *Mater. Chem. Phys.*, 2014, **146**, 113-120.
13. G. S. Machado, O. J. d. Lima, K. J. Ciuffi, F. Wypych and S. Nakagaki, *Catal. Sci. Technol.*, 2013, **3**, 1094-1101.
14. R. De Paula, I. C. M. S. Santos, M. M. Q. Simões, M. G. P. M. S. Neves and J. A. S. Cavaleiro, *J. Mol. Catal. A: Chem.*, 2015, **404–405**, 156-166.
15. G. K. B. Ferreira, K. A. D. d. F. Castro, G. S. Machado, R. R. Ribeiro, K. J. Ciuffi, G. P. Ricci, J. A. Marques and S. Nakagaki, *J. Mol. Catal. A: Chem.*, 2013, **378**, 263-272.
16. S. Kim, K. Y. Lee, Y. S. Lee, H. G. Jang, J. K. Lee and S. J. Lee, *J. Porphyrins Phthalocyanines*, 2014, **18**, 579-584.
17. X. L. Yang and C. D. Wu, *Inorg. Chem.*, 2014, **53**, 4797-4799.
18. J. W. Brown, Q. T. Nguyen, T. Otto, N. N. Jarenwattananon, S. Glöggler and L. S. Bouchard, *Catal. Commun.*, 2015, **59**, 50-54.
19. S. Rayati, P. Jafarzadeh and S. Zakavi, *Inorg. Chem. Commun.*, 2013, **29**, 40-44.
20. V. S. da Silva, L. I. Teixeira, E. do Nascimento, Y. M. Idemori and G. DeFreitas-Silva, *Appl. Catal. A: Gen.*, 2014, **469**, 124-131.
21. K. W. Kwong, T. H. Chen, W. Luo, H. Jeddi and R. Zhang, *Inorg. Chim. Acta*, 2015, **430**, 176-183.
22. Z. Solati, M. Hashemi and L. Ebrahimi, *Catal. Lett.*, 2011, **141**, 163-167.
23. C. G. Sun, B. C. Hu and Z. L. Liu, *Chem. Eng. J.*, 2013, **232**, 96-103.
24. N. Amiri, P. Le Maux, H. Srour, H. Nasri and G. Simonneaux, *Tetrahedron*, 2014, **70**, 8836-8842.
25. J. T. Groves, J. Lee and S. S. Marla, *J. Am. Chem. Soc.*, 1997, **119**, 6269-6273.
26. W. Nam, I. Kim, M. H. Lim, H. J. Choi, J. S. Lee and H. G. Jang, *Chem. Eur. J.*, 2002, **8**, 2067-2071.
27. M. E. Crestoni, S. Fornarini and F. Lanucara, *Chem. Eur. J.*, 2009, **15**, 7863-7866.
28. J. T. Groves and M. K. Stern, *J. Am. Chem. Soc.*, 1987, **109**, 3812-3814.
29. J. T. Groves and M. K. Stern, *J. Am. Chem. Soc.*, 1988, **110**, 8628-8638.
30. R. Latifi, L. Tahsini, B. Karamzadeh, N. Safari, W. Nam and S. P. de Visser, *Arch. Biochem. Biophys.*, 2011, **507**, 4-13.
31. J. T. Groves, Y. Watanabe and T. J. McMurry, *J. Am. Chem. Soc.*, 1983, **105**, 4489-4490.
32. S. E. Park, W. J. Song, Y. O. Ryu, M. H. Lim, R. Song, K. M. Kim and W. Nam, *J. Inorg. Biochem.*, 2005, **99**, 424-431.
33. M. Y. Hyun, Y. D. Jo, J. H. Lee, H. G. Lee, H. M. Park, I. H. Hwang, K. B. Kim, S. J. Lee and C. Kim, *Chem. Eur. J.*, 2013, **19**, 1810-1818.
34. A. J. F. N. Sobral and A. M. D. A. R. Gonsalves, *J. Porphyrins Phthalocyanines*, 2001, **05**, 428-430.
35. A. J. F. N. Sobral and A. M. D. A. R. Gonsalves, *J. Porphyrins Phthalocyanines*, 2001, **05**, 861-866.
36. C. Paliteiro and A. Sobral, *Electrochim. Acta*, 2005, **50**, 2445-2451.
37. M. J. Crossley, P. Thordarson, J. P. Bannerman and P. J. Maynard, *J. Porphyrins Phthalocyanines*, 1998, **02**, 511-516.
38. R. Plamont, Y. Kikkawa, M. Takahashi, M. Kanesato, M. Giorgi, A. Chan Kam Shun, C. Roussel and T. S. Balaban, *Chem. Eur. J.*, 2013, **19**, 11293-11300.
39. Y. Terazono, E. J. North, A. L. Moore, T. A. Moore and D. Gust, *Org. Lett.*, 2012, **14**, 1776-1779.
40. B. Hulsken, R. Van Hameren, J. W. Gerritsen, T. Khoury, P. Thordarson, M. J. Crossley, A. E. Rowan, R. J. M. Nolte, J. A. A. W. Elemans and S. Speller, *Nat. Nanotechnol.*, 2007, **2**, 285-289.
41. S. Zakavi, S. Talebzadeh and S. Rayati, *Polyhedron*, 2012, **31**, 368-372.
42. S. Neya, J. Quan, M. Hata, T. Hoshino and N. Funasaki, *Tetrahedron Lett.*, 2006, **47**, 8731-8732.
43. H. H. Wang, Y. Y. Jiang, M. H. R. Mahmood, H. Y. Liu, H. H. Y. Sung, I. D. Williams and C. K. Chang, *Chin. Chem. Lett.*, 2015, **26**, 529-533.
44. M. P. Trova, P. J. F. Gauuan, A. D. Pechulis, S. M. Bubb, S. B. Bocckino, J. D. Crapo and B. J. Day, *Bioorg. Med. Chem.*, 2003, **11**, 2695-2707.
45. S. H. Peng, M. H. R. Mahmood, H. B. Zou, S. B. Yang and H. Y. Liu, *J. Mol. Catal. A: Chem.*, 2014, **395**, 180-185.
46. O. V. Dolomanov, L. J. Bourhis, R. J. Gildea, J. A. K. Howard and H. Puschmann, *J. Appl. Crystallogr.*, 2009, **42**, 339-341.
47. G. Sheldrick, *Acta Crystallogr. Sect. A*, 2008, **64**, 112-122.
48. F. Paulat, V. K. K. Praneeth, C. Näther and N. Lehnert, *Inorg. Chem.*, 2006, **45**, 2835-2856.
49. G. Canard, D. Gao, A. D'Aléo, M. Giorgi, F. X. Dang and T. S. Balaban, *Chem. Eur. J.*, 2015, **21**, 7760-7771.
50. S. George and I. Goldberg, *Cryst. Growth. Des.*, 2006, **6**, 755-762.

Please do not adjust margins

ARTICLE

51. G. L. Li, J. Nie, H. Chen, Z. H. Ni, Y. Zhao and L. F. Zhang, *Inorg. Chem. Commun.*, 2012, **19**, 66-69.

52. C. Yang, M. Y. Tsai, S. W. Hung, J. H. Chen, S. S. Wang and J. Y. Tung, *Polyhedron*, 2012, **37**, 1-8.

53. J. P. Costes, F. Dahan, B. Donnadieu, M. J. Rodriguez Douton, M. I. Fernandez Garcia, A. Bousseksou and J. P. Tuchagues, *Inorg. Chem.*, 2004, **43**, 2736-2744.

54. M. Araghi, V. Mirkhani, M. Moghadam, S. Tangestaninejad and I. Mohammdpoor-Baltork, *Dalton. Trans.*, 2012, **41**, 3087-3094.

55. Z. Solati, M. Hashemi, S. Hashemnia, E. Shahsevani and Z. Karmand, *J. Mol. Catal. A: Chem.*, 2013, **374–375**, 27-31.

56. S. B. Yang, B. Sun, Z. P. Ou, D. Y. Meng, G. F. Lu, Y. Y. Fang and K. M. Kadish, *J. Porphyrins Phthalocyanines*, 2013, **17**, 857-869.

57. I. Mayer, H. E. Toma and K. Araki, *J Electroanal Chem*, 2006, **590**, 111-119.

58. I. Mayer, M. Nakamura, H. E. Toma and K. Araki, *Electrochim. Acta*, 2006, **52**, 263-271.

59. J. Haber, L. Matachowski, K. Pamin and J. Poltowicz, *J. Mol. Catal. A: Chem.*, 2003, **198**, 215-221.

60. Z. M. Zhang, L. Ouyang, W. Q. Wu, J. X. Li, Z. C. Zhang and H. F. Jiang, *J. Org. Chem.*, 2014, **79**, 10734-10742.

61. M. Zhao, S. Ou and C. D. Wu, *Acc. Chem. Res.*, 2014, **47**, 1199-1207.

62. Q. Wang, Y. Zhang, L. Yu, H. Yang, M. H. Mahmood and H. Y. Liu, *J. Porphyrins Phthalocyanines*, 2014, **18**, 316-325.

63. F. G. Doro, J. R. L. Smith, A. G. Ferreira and M. D. Assis, *J. Mol. Catal. A: Chem.*, 2000, **164**, 97-108.

64. A. N. Biswas, A. Pariyar, S. Bose, P. Das and P. Bandyopadhyay, *Catal. Commun.*, 2010, **11**, 1008-1011.

65. E. T. Saka, D. Çakır, Z. Bıyıklıoğlu and H. Kantekin, *Dyes Pigment.*, 2013, **98**, 255-262.

66. L. J. Boucher, *J. Am. Chem. Soc.*, 1970, **92**, 2725-2730.

67. L. J. Boucher, *Coord. Chem. Rev.*, 1972, **7**, 289-329.

68. H. Y. Liu, T. S. Lai, L. L. Yeung and C. K. Chang, *Org. Lett.*, 2003, **5**, 617-620.

69. N. Jin and J. T. Groves, *J. Am. Chem. Soc.*, 1999, **121**, 2923-2924.

70. W. Y. Zhou, P. Tian, Y. Chen, M. Y. He, Q. Chen and Z. X. Chen, *Bioorg. Med. Chem. Lett.*, 2015, **25**, 2356-2359.

71. T. B. Li, G. Chen, C. Zhou, Z. Y. Shen, R. C. Jin and J. X. Sun, *Dalton. Trans.*, 2011, **40**, 6751-6758.

Please do not adjust margins

RSC Advances

ARTICLE
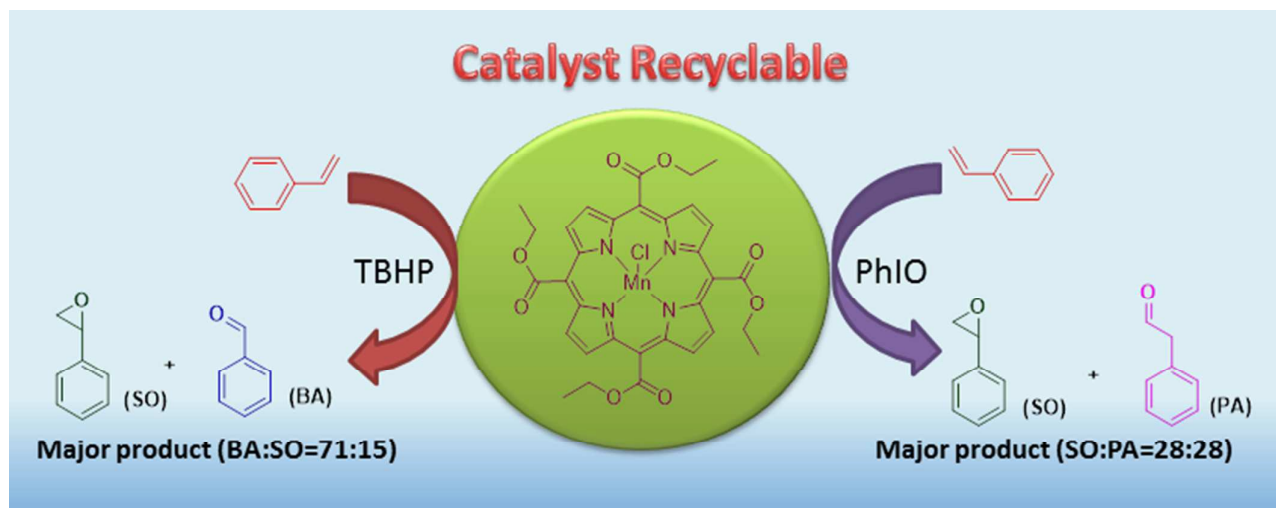
Single crystal structure revealed 5,10,15,20-tetrakis(ethoxycarbonyl)porphyrin manganese(III) chloride (Mn[III]TECPCl) existed as a Mn–O coordinated dimer having a weak antiferromagnetic Mn(III) - Mn(III) coupling. In the catalytic oxidation of styrene using TBHP or PhIO oxidant under atmosphere, Mn[III]TECPCl gave high yield of oxidantion products and was found recyclable.